Mechanical Testing Results on Core from Borehole U-15n, NNSS, in support of SPE

Scott Broome[1] and Tom Pfeifle[2],
[1]Geomechanics (08864), [2]Energetic Component Engineering 1 (02552)
Sandia National Laboratories
PO Box 5800, MS 1033
Albuquerque, New Mexico 87185-1033

Abstract

The Nevada National Security Site (NNSS) will serve as the geologic setting for a Source Physics Experiment (SPE) program. The SPE will provide ground truth data to create and improve strong ground motion and seismic S-wave generation and propagation models. The NNSS was chosen as the test bed because it provides a variety of geologic settings ranging from relatively simple to very complex.

Each series of SPE testing will comprise the setting and firing of explosive charges (source) placed in a central bore hole at varying depths and recording ground motions in instrumented bore holes located in two rings around the source positioned at different radii. Modeling using advanced simulation codes will be performed both *a priori* and after each test to predict ground response and to improve models based on acquired field data, respectively.

A key component in the predictive capability and ultimate validation of the models is the full understanding of the intervening geology between the source and the instrumented bore holes including the geomechanical behavior of the site rock/structural features. This report presents a limited scope of work for an initial phase of primarily unconfined compression testing.

Samples tested came from the U-15n core hole, which was drilled in granitic rock (quartz monzonite). The core hole was drilled at the location of the central SPE borehole, and thus represents material in which the explosive charges will be detonated. The U-15n location is the site of the first SPE, in Area 15 of the NNSS.

Sample Preparation and Experimental Methods

Specimen Preparation: Test specimens (right circular cylinders) were prepared from the 2.5-in-dia field core by cutting them to approximate length using a standard rock saw and then grinding the ends flat and parallel to final length such that the length-to-diameter ratio, L:D, on each test specimen is 2:1. Both the sawing and the grinding used standard tap water for cooling. All specimen dimensions were sized to provide representative results given the maximum grain size of this granite ranges from 0.5-6.35 mm (0.02-0.25 in). Phenocrysts in small quantities were observed along the core length and are as large as ~25.4 mm across. The dimensions and mass of each specimen were accurately measured. Field cores used in preparing the test specimens were selected from approximately every 20-foot interval of U-15n and had a useable length of approximately 6-7 inches so that the 5-inch-long specimens were prepared with sufficient

material available near one end of each core to obtain thin sections and/or thicker billets of untested rock.

Calibration: Annual calibration of the load cell used to calculate unconfined compressive strength (UCS) is traceable to the U.S. National Institute of Standards and Technology. For all UCS tests, two strain gages were bonded at sample mid-height 180° apart. A shakedown test was performed with a right circular steel specimen (4340 steel) instrumented with the same strain gages as those used on the SPE granite samples prior to any SPE UCS testing. The shake down test verified that all components of the test system were functioning correctly by ensuring measured properties (Young's modulus and Poisson's ratio) matched those published for 4340 steel.

Bulk Density Determination: The bulk density of each UCS test specimen was determined from its mass and volume where volume is calculated using dimensional measurements assuming a right-circular-cylindrical geometry.

Unconfined Compressive Strength (UCS) Testing: UCS tests were performed on granite specimens prepared from field cores recovered from approximately every 20-foot interval of U-15n. Using this strategy, tests were run on what is thought to be both weathered and fresh granite to determine if there are differences in mechanical properties over the entire core hole depth (~200 ft). All specimens were instrumented to measure axial stress and axial and radial strains and were loaded quasi-statically in compression (axial strain rate of $\sim 1 \times 10^{-4}$/sec) under ambient pressure and temperature conditions. Loading continued until the peak axial stress (i.e., the UCS strength) was observed. All samples were loaded to failure. However during loading, unload/reload cycles were performed at various axial stress levels to acquire data to estimate the compressive elastic properties – Young's modulus, E_c, and Poisson's ratio, ν_c.

Compressional and Shear Wave Velocity Measurements: Ultrasonic compressional and shear wave velocity measurements, V_p and V_s, were performed on each UCS specimen under ambient conditions prior to UCS testing. Wave speed measurements were made coincident with each specimen axis and also orthogonal to the axis across two diameters separated by 90^0.

Experimental Results

Table 1 lists the results from the unconfined compressive strength tests for borehole U-15n. Included in Table 1 are the sample number, depth, density, maximum axial stress (i.e., UCS strength), Young's modulus, Poisson's ratio and failure mode. Elastic properties were determined from the average of the unload portion of two unload/reload loops performed while the sample was loaded at a constant axial strain rate of ~1E-04. Elastic properties for Sample SPE-UCS-5 were averaged from the slope during initial loading and one unload/reload cycle. Only one strain gage was used for the unload/reload cycle for this sample because the other strain gage had started to fail producing erratic data. This sample failed at the lowest stress and was from a highly altered zone adjacent to a fault. The failure mode for all samples was intact except for SPE-UCS-10. The failure mode for this sample was primarily along a pre existing

weakness plane with a failure surface angle of ~79° where 0° is perpendicular to the core axis. Samples with an intact failure mode nominally failed at angles between 70° to 80° resulting in a fairly intact cone on either end of the sample.

Table 1. Sample #, Depth, Density, UCS Strength, Young's modulus, Poisson's Ratio and Failure Mode for U-15n

Sample	Depth (ft)	Density (g/cc)	$\sigma_{AX,\,MAX}$ (MPa)	*E* (GPa)	*v*	Failure Mode[1]
SPE-UCS-1	14	2.65	235.6	75.94	0.254	Intact
SPE-UCS-2*	29	2.61	121.1	56.28	0.248	Intact
SPE-UCS-3	50	2.64	226.5	77.63	0.236	Intact
SPE-UCS-4	70	2.63	184.3	64.26	0.245	Intact
SPE-UCS-5**	87	2.55	41.6	35.07	0.16	Intact
SPE-UCS-6	108	2.64	210.2	70.28	0.218	Intact
SPE-UCS-7	132	2.63	205.4	76.4	0.201	Intact
SPE-UCS-8	154	2.64	192.8	75.67	0.232	Intact
SPE-UCS-9	177	2.64	227.8	77.79	0.24	Intact
SPE-UCS-10	192	2.65	165.8	76.38	0.22	Intact/Fracture

[1] Intact failure mode indicates failure through intact material rather than along planes of weakness
*Sample designated as weathered granite
**Sample from a highly altered zone adjacent to a fault. Elastic properties determined from initial loading and one unload/reload loop from one strain gage near failure

Sample SPE-UCS-9 had a chip on the top edge (Figure 1). It was decided to test the sample with the chip rather than cut it shorter and violate the 2:1 length-to-diameter ratio criterion. This sample failed at the highest stress and thus the chip was not likely to have significantly altered the UCS strength. Figure 2 shows a typical sample, complete with strain gages, mounted in the 5 MN load frame. The plastic curtain surrounding the loading platens ensured most tested pieces of the sample could be retained in the event of catastrophic failure. Plots of Engineering Axial Stress versus Axial, Lateral, and Volume strain for all ten UCS tests are presented at the end of report SAND2011-4394C. Volumetric strain is calculated from the axial and radial strains, i.e., $\varepsilon_v = \varepsilon_{ax} + 2\varepsilon_{rad}$.

Tables 2, 3 and 4 list the results from ultrasonic compressional and shear wave velocity measurements taken coincident with each specimen axis and also orthogonal to the axis across two diameters separated by 90° respectively. The S Wave parallel to the core axis for sample SPE-UCS-3 was ambiguous and *v* dynamic is not reported. Figure 3 shows a typical voltage versus time plot used to determine P and S wave velocities.

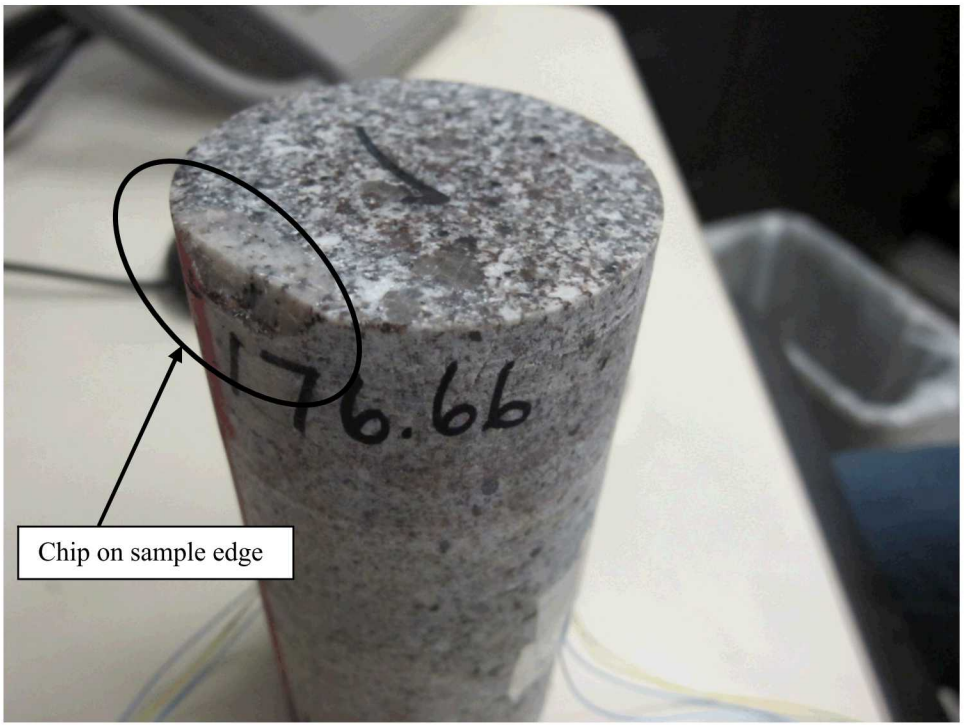

Figure 1. Sample SPE-UCS-9 with a chip on the top edge.

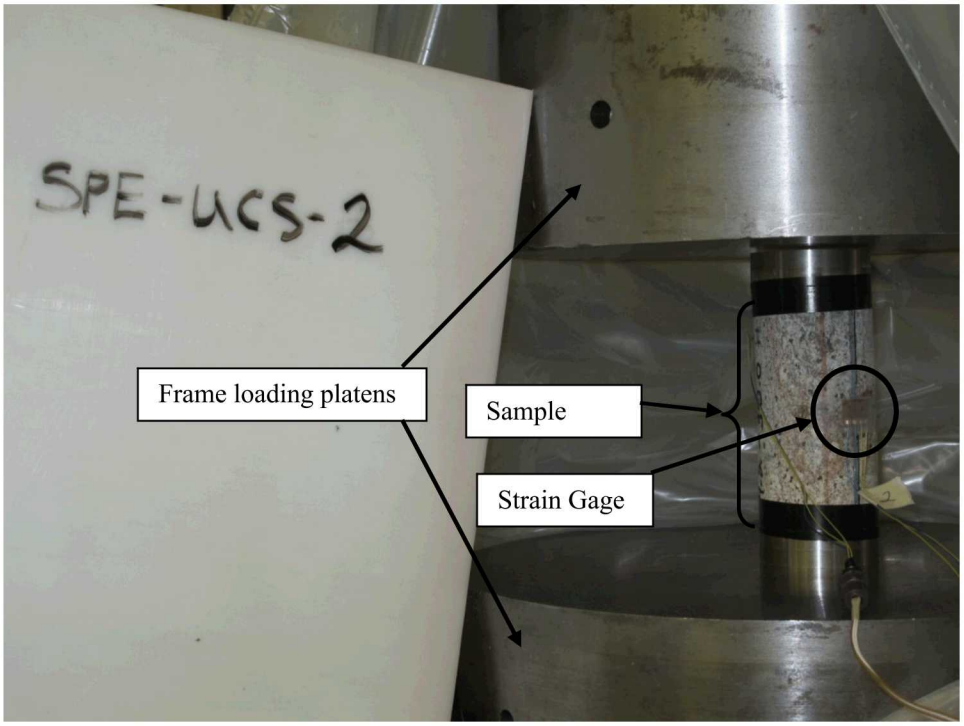

Figure 2. Sample SPE-UCS-2 mounted in load frame.

Table 2. P- and S-wave travel time and velocity and calculated values of dynamic *E* and *v* along core axis

	Axial					
Sample #	P Wave Travel Time (µs)	P-Velocity (mm/µs)	S-Wave Travel Time (µs)	S-Velocity (mm/µs)	$E_{Dynamic}$ (GPa)	$v_{Dynamic}$
SPE-UCS-1	22.02	5.8344	37.24	3.4325	77.01	0.235
SPE-UCS-2	27.44	4.6883	43.36	2.9562	53.40	0.170
SPE-UCS-3*	21.19	6.1132	29.01	4.4499	97.94	N/A*
SPE-UCS-4	22.55	5.7025	36.55	3.5020	77.22	0.197
SPE-UCS-5	26.44	4.8752	40.59	3.1643	58.11	0.136
SPE-UCS-6	22.20	5.8016	36.36	3.5253	79.23	0.207
SPE-UCS-7	22.08	5.8195	36.53	3.5004	78.41	0.217
SPE-UCS-8	21.79	5.9275	37.26	3.4485	78.25	0.244
SPE-UCS-9	22.09	5.8879	38.43	3.3667	75.33	0.257
SPE-UCS-10	21.90	5.9079	36.03	3.5735	81.86	0.212

*For Axial direction on sample SPE-UCS-3, S Wave was ambiguous

Table 3. P- and S-wave travel time and velocity and calculated values of dynamic *E* and *v* orthogonal to core axis (along red line on core)

	Radial - 0°					
Sample #	P-Wave Travel Time (µs)	P-Velocity (mm/µs)	S-Wave Travel Time (µs)	S-Velocity (mm/µs)	$E_{Dynamic}$ (GPa)	$v_{Dynamic}$
SPE-UCS-1	11.64	5.5804	18.96	3.3948	73.56	0.206
SPE-UCS-2	14.19	4.5381	22.54	2.8365	49.56	0.179
SPE-UCS-3	10.47	6.1757	17.73	3.6078	85.31	0.241
SPE-UCS-4	11.43	5.6718	18.32	3.5067	77.00	0.191
SPE-UCS-5	14.16	4.5552	21.81	2.9374	50.43	0.144
SPE-UCS-6	11.04	5.8819	18.35	3.5037	79.41	0.225
SPE-UCS-7	10.95	5.9386	17.2	3.7462	86.33	0.170
SPE-UCS-8	11.18	5.8110	18.14	3.5478	80.07	0.203
SPE-UCS-9	10.82	6.0165	16.88	3.8215	89.71	0.162
SPE-UCS-10	11.04	5.8960	18	3.5815	81.97	0.208

Table 4. P- and S-wave travel time and velocity and calculated values of dynamic *E* and *v* orthogonal to core axis (perpendicular to red line on core)

	Radial - 90°					
Sample #	P-Wave Travel Time (µs)	P-Velocity (mm/µs)	S-Wave Travel Time (µs)	S-Velocity (mm/µs)	$E_{Dynamic}$ (GPa)	$\nu_{Dynamic}$
SPE-UCS-1	11.56	5.6199	18.56	3.4691	75.91	0.192
SPE-UCS-2	14.53	4.4299	22.8	2.8038	47.87	0.166
SPE-UCS-3	10.42	6.2061	17.6	3.6349	86.45	0.239
SPE-UCS-4	11.42	5.6768	18.78	3.4196	74.74	0.215
SPE-UCS-5	13.77	4.6868	21.3	3.0086	53.15	0.150
SPE-UCS-6	11.22	5.7852	18.74	3.4298	76.34	0.229
SPE-UCS-7	10.91	5.9609	18.46	3.4867	79.29	0.240
SPE-UCS-8	11.16	5.8217	18.51	3.4758	78.14	0.223
SPE-UCS-9	10.95	5.9433	17.14	3.7626	87.24	0.166
SPE-UCS-10	11.01	5.9125	17.25	3.7397	86.33	0.167

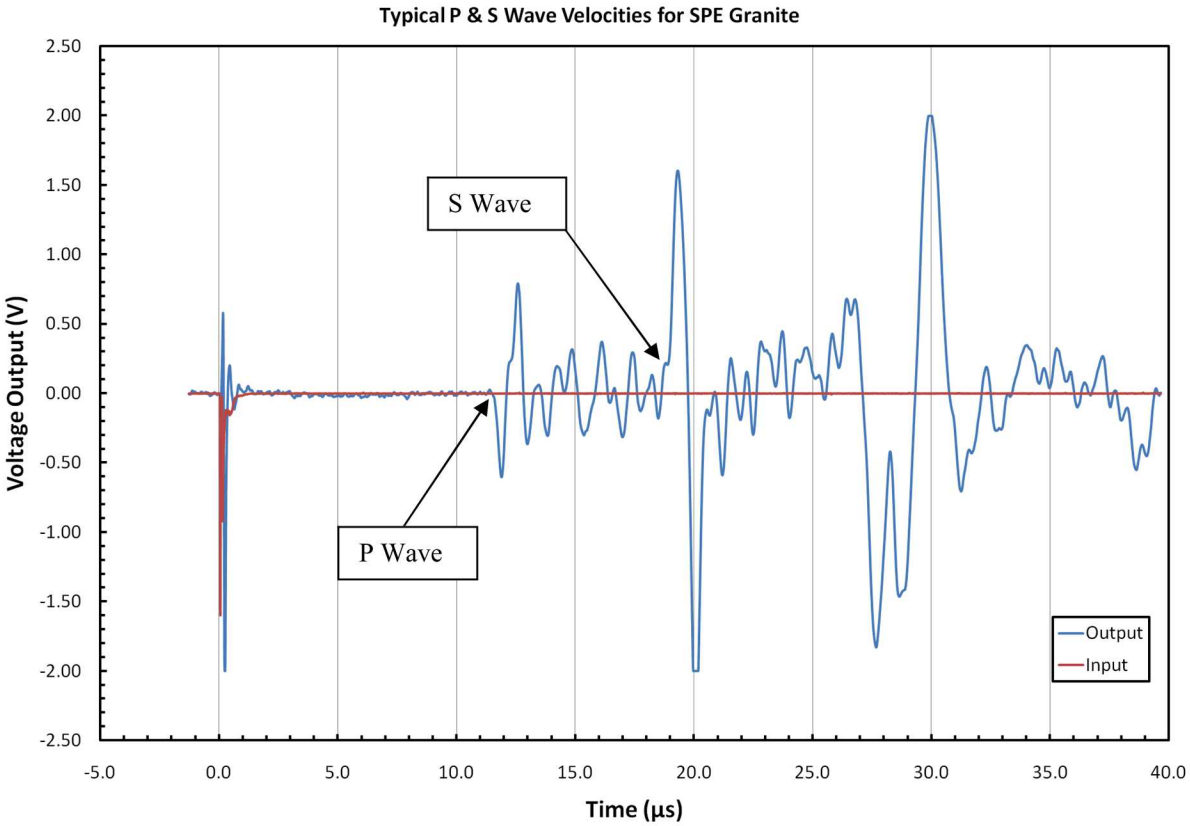

Figure 3. Typical velocity profile for determination of P & S wave speed.

The dynamic elastic Young's modulus, $E_{dynamic}$, was determined directly from:

$$E_{dynamic} = \frac{\rho V_S^2 \left(3V_P^2 - 4V_S^2\right)}{\left(V_P^2 - V_S^2\right)}$$

Where ρ is the sample density and V_P and V_S are the compressional and shear wave velocities, respectively. Values of dynamic elastic Poisson's ratio, $\nu_{dynamic}$, were calculated from:

$$\nu_{dynamic} = \frac{\left(V_P^2 - 2V_S^2\right)}{2\left(V_P^2 - V_S^2\right)}$$

Dynamic Young's modulus ranges from approximately 47.9 to 97.9 GPa and Poisson's ratio ranges from approximately 0.14 to 0.26 for all samples measured in the axial direction.

Analysis of Results

Figure 4 plots density, unconfined compressive strength, Young's modulus and Poisson's ratio as functions of depth. Density is reasonably uniform over the cored interval, i.e., ~2.63 g/cc, with the exception of two depths, -29 ft and -87 ft where it decreases slightly to 2.61 g/cc and somewhat more to 2.55 g/cc. Unconfined compressive strength, Young's modulus and Poisson's ratio follow this trend. The unconfined compressive strength is nominally 200 MPa or greater over the cored depth; however, at depths of -29 ft, -87 ft and -192 ft, the strength drops off to 121, 42 and 166 MPa, respectively.

As discussed above, Young's modulus was determined using two methods: 1) directly from stress-strain data acquired during quasi-static unload/reload cycles and 2) indirectly calculated from density and compressional and shear wave velocity measurements. The values of Young's Modulus determined from the quasi-static testing were nominally 76 GPa with lower values found from cores recovered at depths of -29 ft (56 GPa) and -87 ft (35 GPa). The values determined indirectly (dynamic methods) were consistently higher than the quasi-static values as expected except for cores recovered from near the surface (-14 ft and -29 ft). For the deeper cores, the dynamic moduli were about 5 to 20% higher than the quasi-static values except at a depth of -87 ft where the dynamic modulus was about 50% higher. There was no observable difference in Poisson's ratio using either the quasi-static or dynamic methods. In general, the values of Poisson's ratio (both measured quasi-statically and dynamically) ranged from about 0.15 to 0.25.

Compressional and shear wave velocities are plotted as a function of depth for measurements made parallel (axial) and normal (radial) to the specimen central axis in Figure 5. With the

exception of measurements made at depths of -29 ft and -87 ft, compressional wave velocities are ~5,900 m/sec. At -29 ft and -87 ft, the compressional wave velocities are ~4,500 m/sec and ~4,700 m/sec, respectively. The shear wave velocities are ~3,600 m/sec but drop somewhat at -29 ft and -87 ft to ~2,900 m/sec and ~3,000 m/sec, respectively. Within the variability of the measurements, it appears there is no significant difference in velocities when measured parallel or normal to the specimen axis implying the recovered cores are reasonably isotropic (from a mechanical point of view).

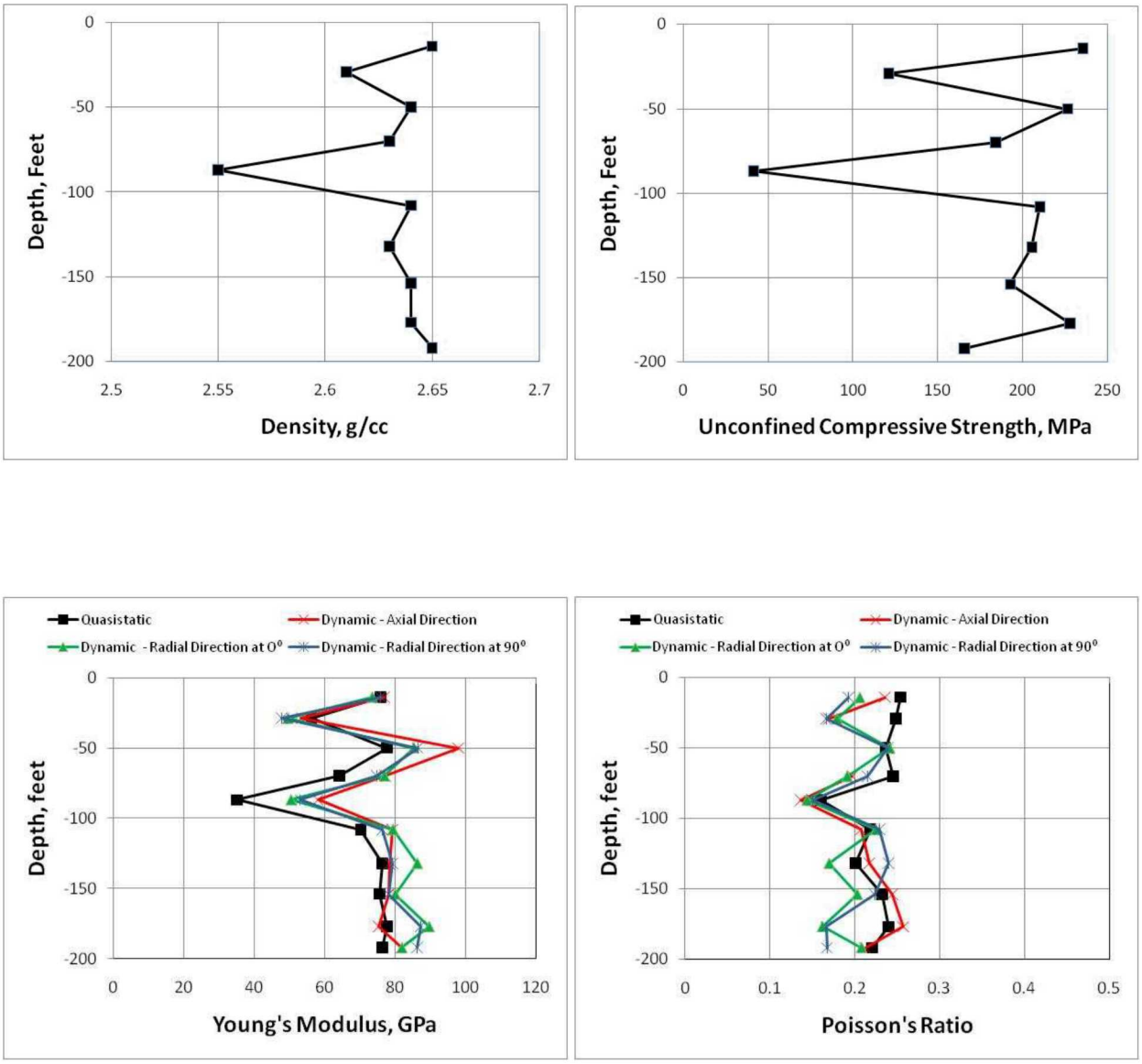

Figure 4. Density, UCS strength, Young's modulus and Poisson's ratio as functions of depth for Borehole U15-n.

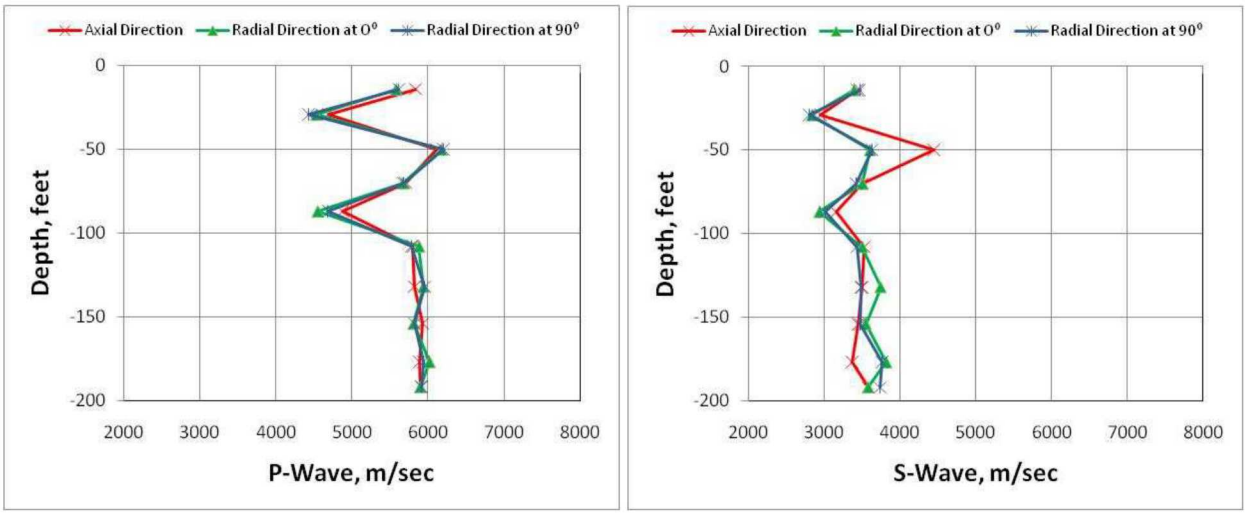

Figure 5. Compressional and shear wave velocities as functions of depth for Borehole U15-n.

A limited literature search was conducted to find relevant data sets that could be used for comparison with data acquired under this testing program. Schock et al (1973) published data from quasi-static tests conducted on granodiorite samples recovered from the Climax stock, Area 15, Nevada National Security Site, Nye County, Nevada. Tests included hydrostatic compression to 4 GPa, triaxial compression at various confining pressures up to 700 MPa and uniaxial strain. The granodiorite tested in their study had a material density of 2.67 g/cc and a porosity of ~0.7%. Although Schock et al did not conduct any unconfined tests, they did perform one test at a confining pressure of 1 bar (0.1MPa). From plots presented in their paper, estimates of compressive strength, Young's modulus and Poisson's ratio were determined to be ~220 MPa, 60 GPa and 0.2-0.3, respectively. These values are in reasonably good agreement with those determined from the current study if values from depths of -29 ft and -87 ft are not used in the comparison. Wilder and Yow (1987) presented data acquired from tests on Climax stock samples comprising granodiorite and quartz monzonite and also summarized data from Pratt el al. The quartz monzonite tested in this second study had a density of 2.635 g/cc and a porosity of 3.2%. Properties reported in this study for UCS strength, Young's modulus and Poisson's ratio were 200 MPa, 48 GPa, and 0.21. With the exception of Young's modulus which is somewhat lower than in the current study, these properties compare favorably with those measured in the current study, again assuming the values obtained at depths of -29 ft and -87 ft are not used in the comparison. Wilder and Yow also reported a dynamic Young's modulus of 82.8 GPa, and compressional and shear wave velocities of 6,058 m/sec and 3,541 m/sec, respectively, all of which are in very good agreement with the current study (with the exception of properties measured at depths of -29 ft and -87 ft). Both data sets presented in the referenced reports are from depths of 942 ft (HARD HAT) to 1519 ft (PILE DRIVER) below ground surface; deeper than the current tested range of 14 ft to 192 ft.

Contents of this report taken from Broome (2011). Broome (2011) contains additional figures, tables, additional discussion of results, and appendices with details of individual tests.

References

Broome, S. and Pfeifle, T., 2011. Phase 1 Mechanical Property Test Results for Borehole U-15n in Support of NCNS Source Physics Experiment, SAND2011-4394C.

Schock, R.N., H.C. Heard, and D.R. Stephens, 1973. "Stress-Strain Behavior of a Granodiorite and Two Graywackes in Compression to 20 Kilobars," *J. of Geophysical Research*, Vol 78, No. 26, September.

Wilder, D.G. and J.L. Yow, Jr., 1987. "Geomechanics of the Spent Fuel Test – Climax," UCRL-53767, prepared by Lawrence Livermore National Laboratory, Livermore, CA, July.

Sandia National Laboratories is a multimission laboratory managed and operated by National Technology and Engineering Solutions of Sandia, LLC, a wholly owned subsidiary of Honeywell International, Inc., for the U.S. Department of Energy's National Nuclear Security Administration under contract DE-NA0003525.